Electron Microscopy I
Lecture 10

TT.Prof. Dr. Yolita M. Eggeler

Laboratory for electron microscopy,
CFN building, 2nd floor, room 215
yolita.eggeler@kit.edu
Phone 608-43724

Laboratory for Electron Microscopy

Electron Microscopy I

Laboratory for Electron Microscopy

Conventional and convergent electron diffraction

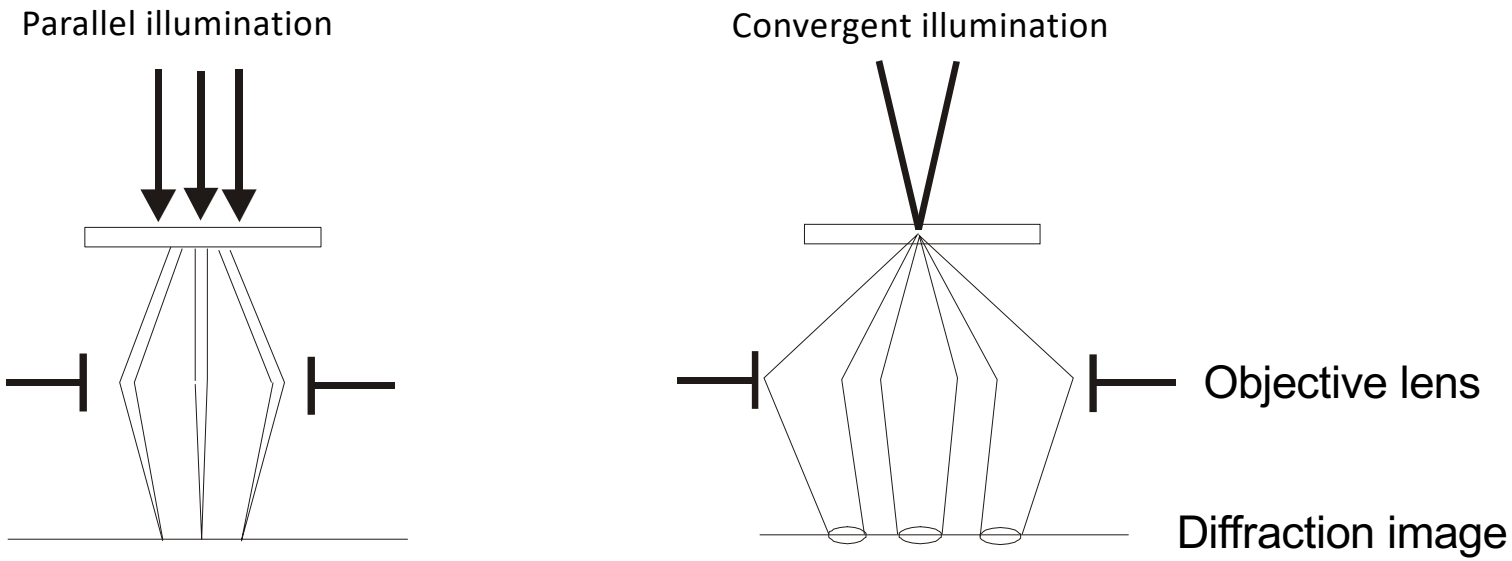

Conventional electron diffraction: parallel illumination / point-like Bragg reflections

Convergent electron diffraction: convergent illumination / slice-shaped diffraction stretched reflexes

Parallel illumination:
Selection of small sample areas with fine range aperture or in nano-diffraction mode

Convergent illumination:
Selection of small sample areas by focusing the electron beam on small Diameter

4.6 Diffraction patterns / Convergent electron diffraction

Laboratory for Electron Microscopy

Single crystal

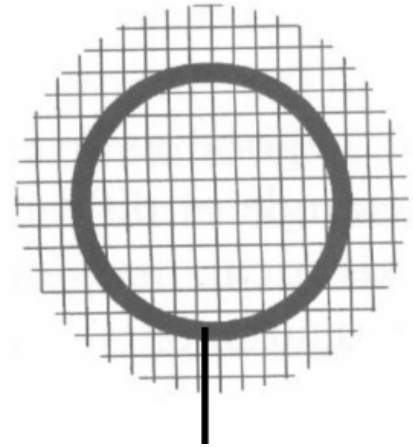

Fine range aperture

Regular points arrangement

Polycrystalline (coarse grains)

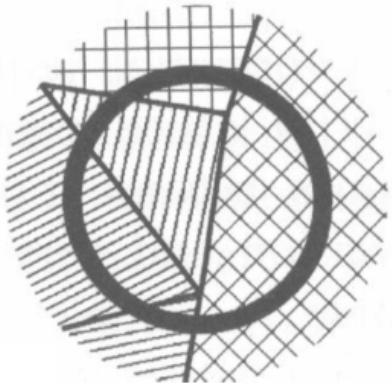

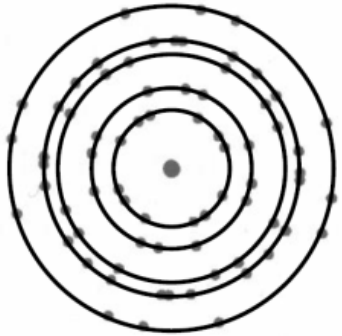

Dots arranged on rings

Polycrystalline (small grains)

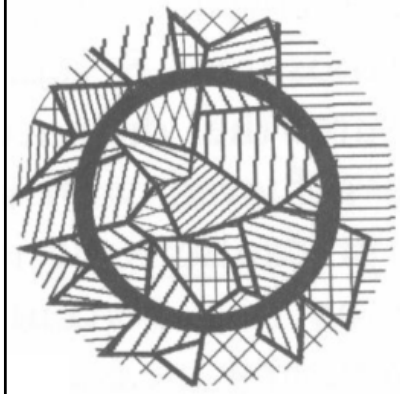

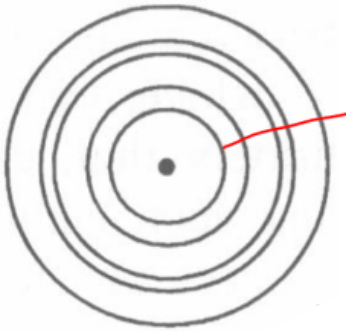

Rings

Laboratory for Electron Microscopy

Example: Diffraction of monocrystalline gold vs. polycrystalline gold

Single crystal diffraction
of Au in [001] zones axis

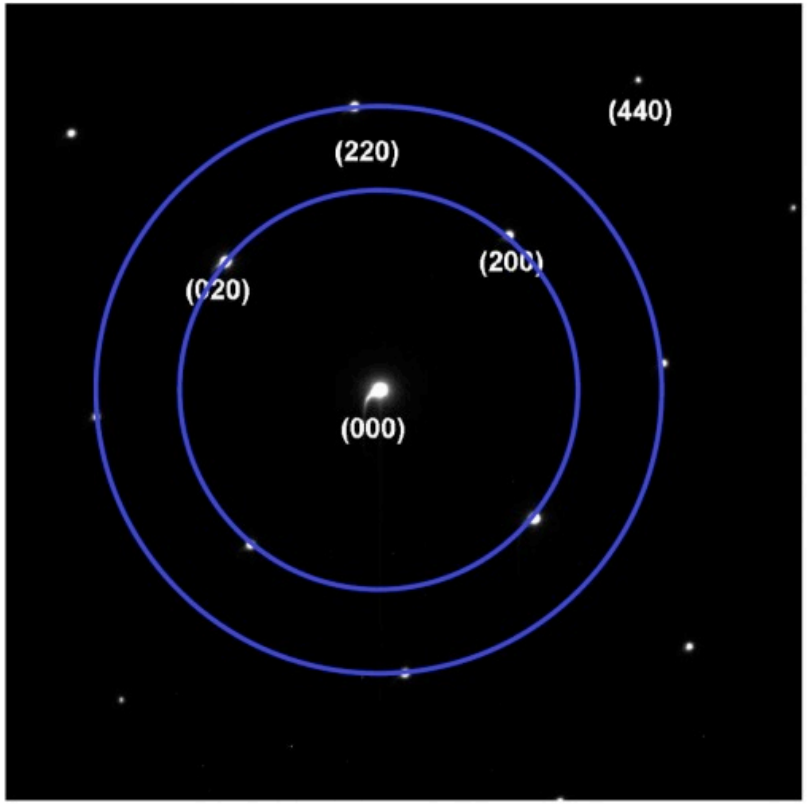

Polycrystal Diffraction of Au

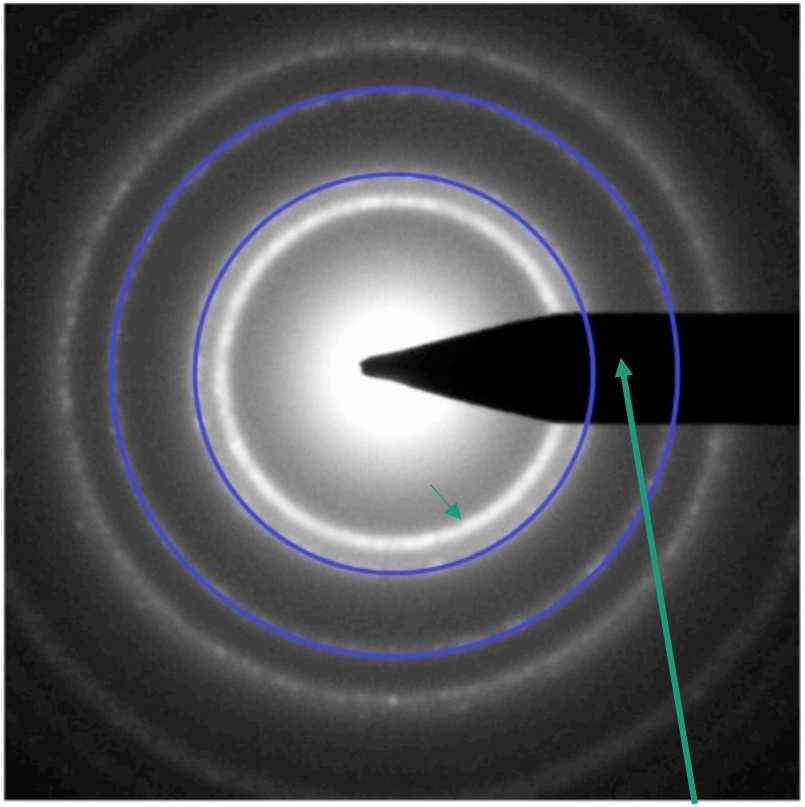

Beamstop: prevents the high intensity of the primary beam from damaging the CCD camera.

Laboratory for Electron Microscopy

Conventional diffraction: polycrystalline / nanocrystalline samples

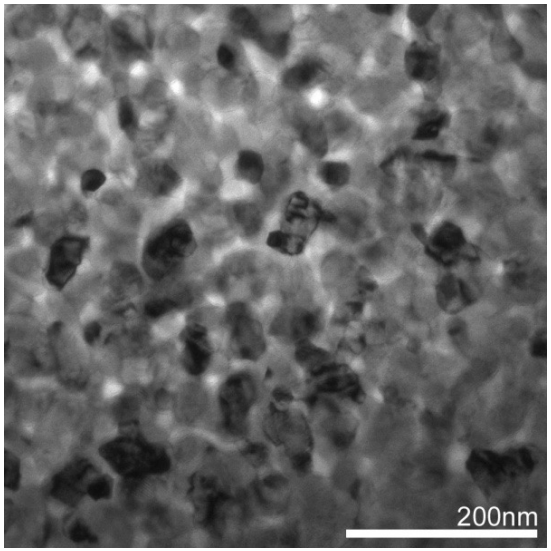

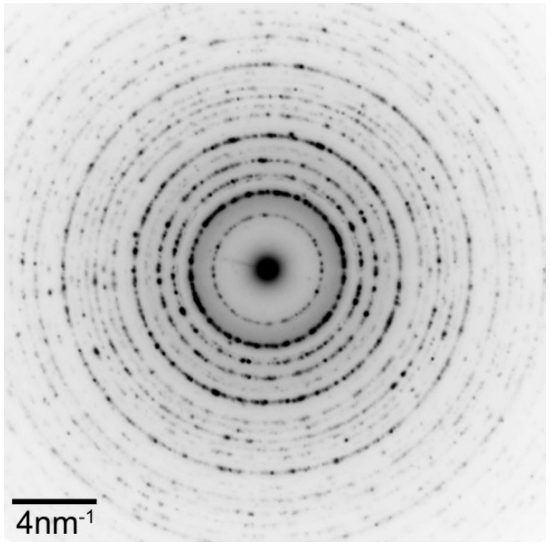

Debye diffraction images:

- Arrangement of the reflexes on rings
- Number of reflexes on rings depending on the number of grains recorded

Inverted contrast of the diffraction image

L. Dieterle, LEM 2006

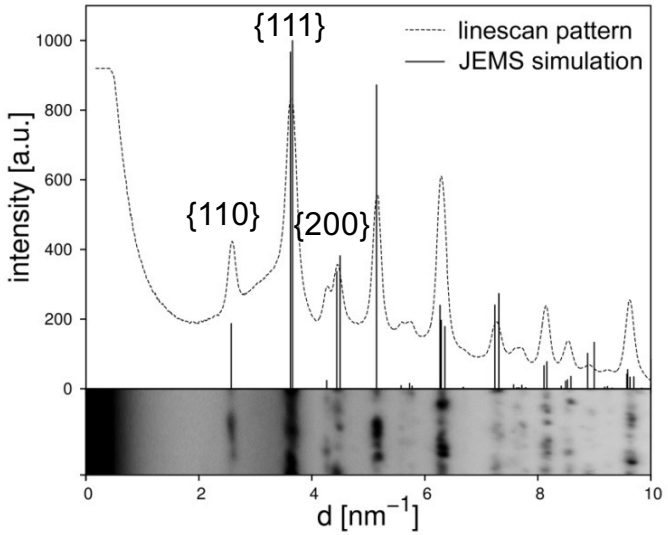

Rings correspond to kinematically permitted Bragg Reflexes

$(La_{0.5}\ Sr_{0.5})MnO_3$

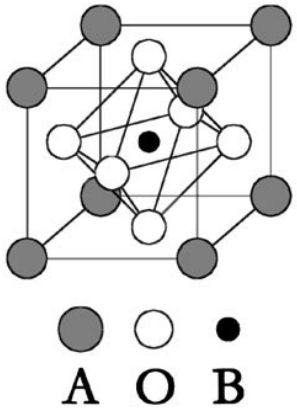

Laboratory for Electron Microscopy

Conventional diffraction: amorphous materials

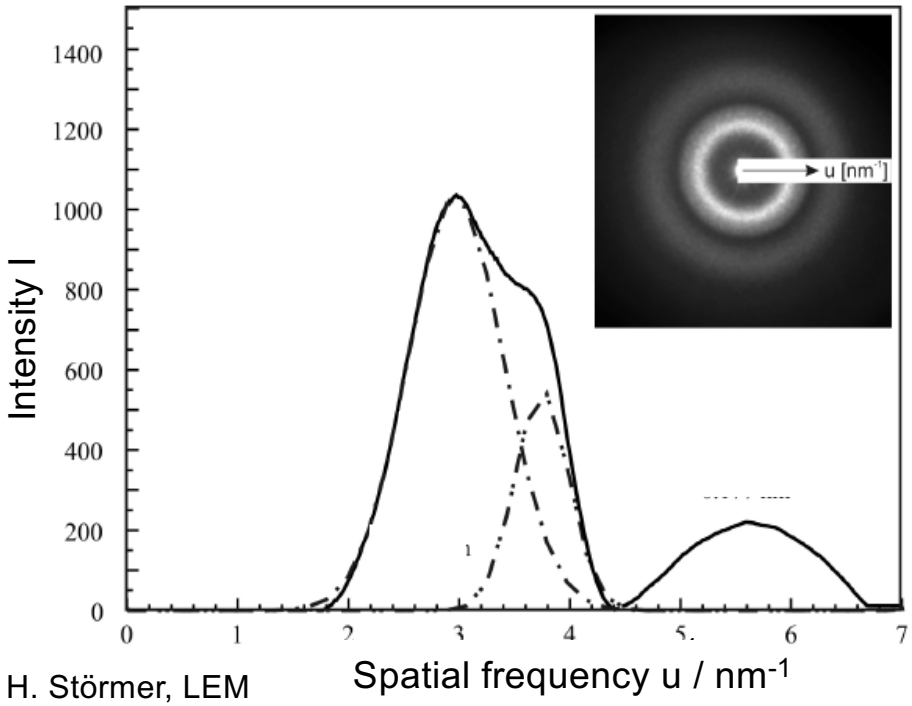

H. Störmer, LEM

Diffraction pattern of amorphous Nb O_{25}

Diagram of pair correlation function G(r)

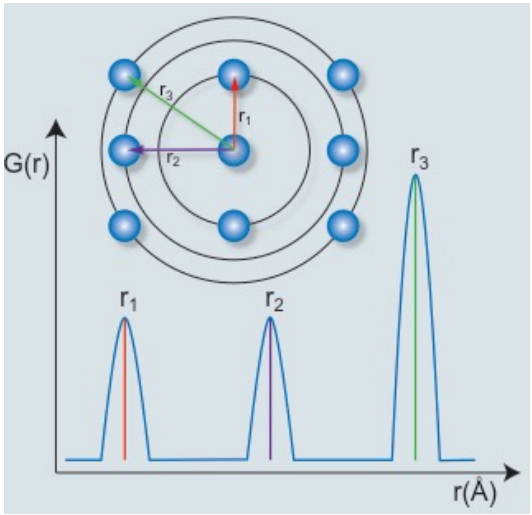

- There are diffusely widened rings, due to a certain degree of close order symmetry in amorphous materials.
- Ring positions in diffraction images of amorphous materials are determined by the pair correlation function G(r), which indicates the probability of finding a neighboring atom at a certain distance r
- G(r) is obtained by Fourier transformation of the measured intensity I(u) after suitable background subtraction (see e.g. J. Appl. Cryst. 50, 304 (2017))

4.6 Diffraction patterns / Convergent electron diffraction

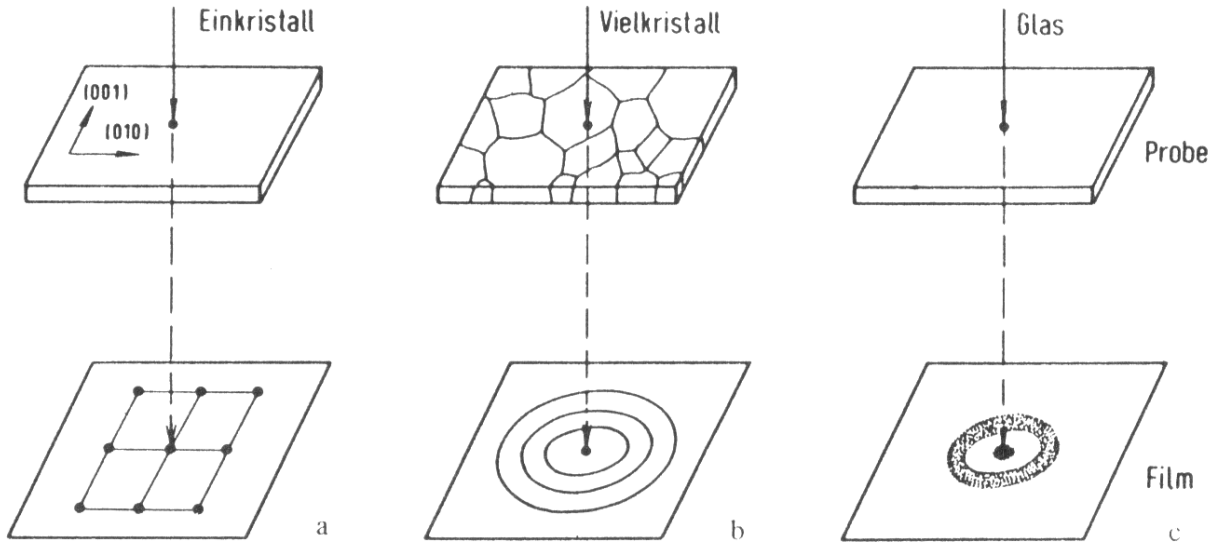

Abb. 3.4: Schematische Darstellung der Beugungsbilder. a) Einkristall → Punktdiagramm b) Vielkristall → Ringdiagramm mit scharfen Ringen c) Amorpher Festkörper → wenige diffuse Ringe

E. Hornbogen, B. Skrotzki, Materials microscopy, Fig. 3.4

Poly/nanocrystalline → amorphous materials:
Widening of the rings with sharp reflections to diffuse rings
Decrease in the number of rings

Laboratory for Electron Microscopy

Convergent diffraction (CBED: convergent beam electron diffraction)

Information from small sample areas
determined by beam diameter
and beam expansion in the sample

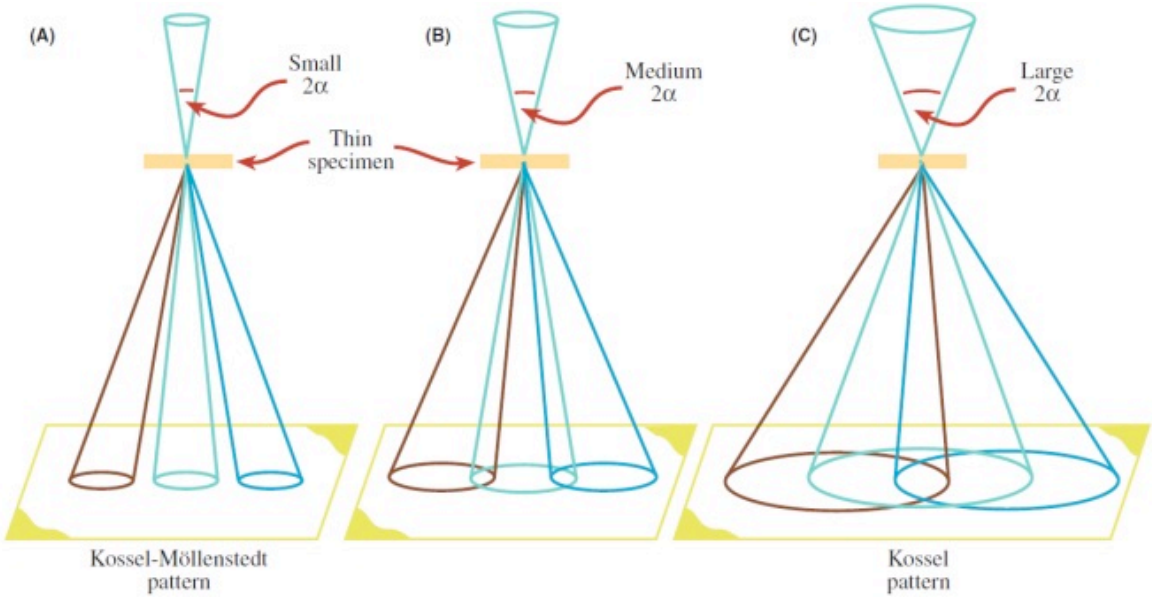

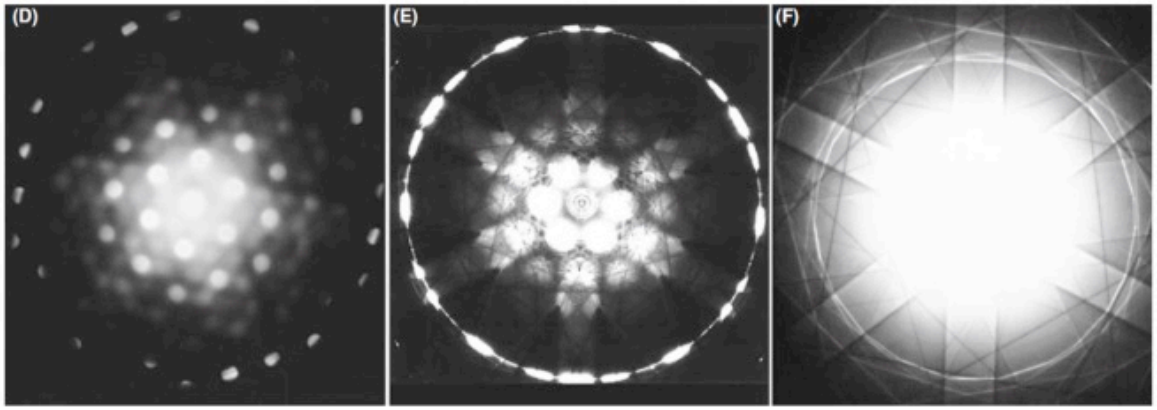

FIGURE 20.3. (A–C) Ray diagrams showing how increasing the C2 aperture size causes the CBED pattern to change from one in which individual disks are resolved (K-M pattern) to one in which all the disks overlap (Kossel pattern). (D–F) You can see what happens to experimental CBED patterns on the TEM screen as you select larger C2 apertures.

D.B. Williams, C.B. Carter,
Transmission Electron Microscopy,
Fig. 20.3

Laboratory for Electron Microscopy

CBED under dual beam conditions

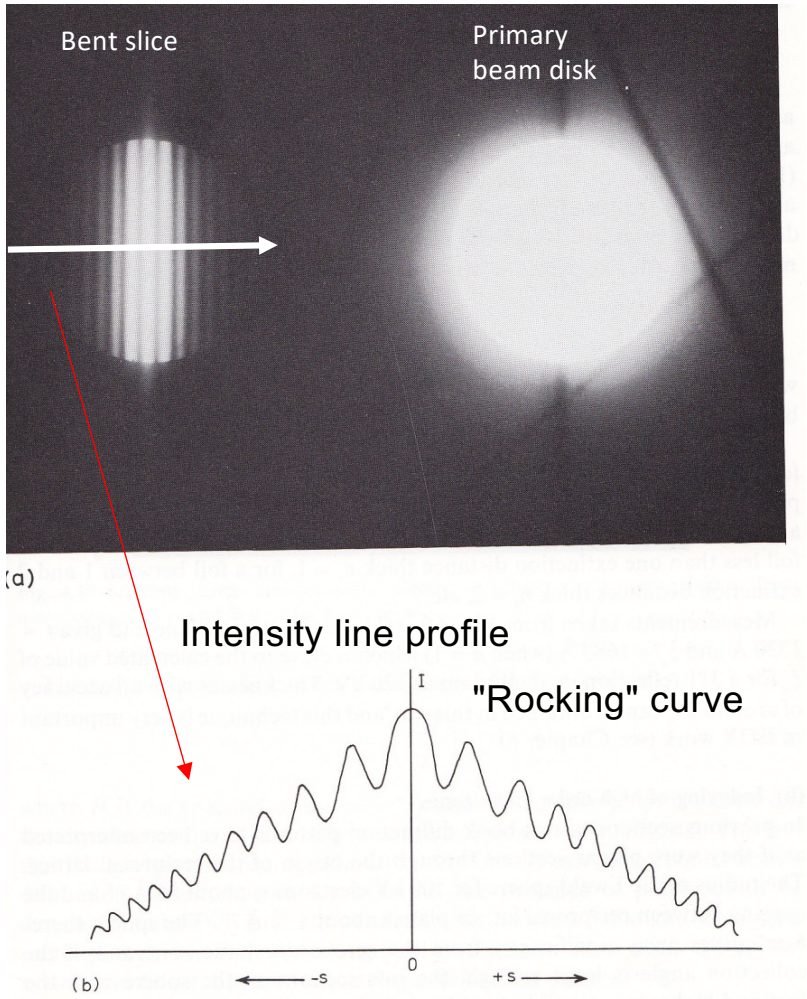

Fig. 4.9 (a) Magnified image of a convergent beam diffraction pattern taken from aluminium at 120 kV. The diffracted beam shows minima corresponding to those in (b). The precise positions of the minima depend on the foil thickness (cf. equation (4.5)).

M.H. Loretto, Electron Beam Analysis of Materials, p.81

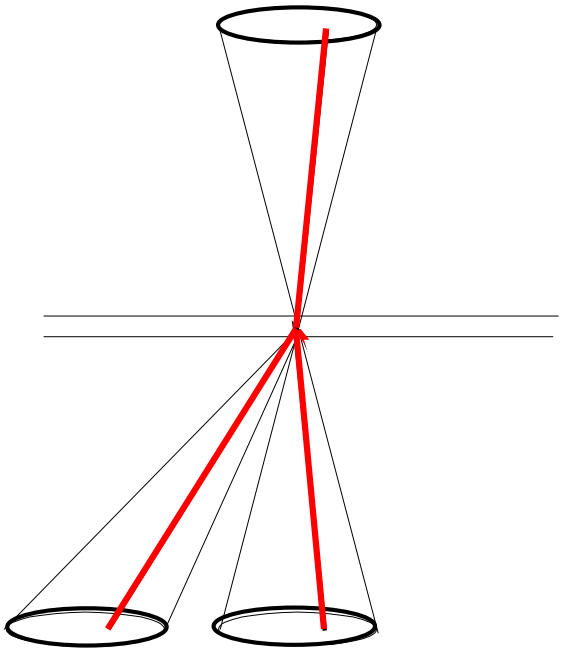

- The intensity distribution in the diffraction disk is determined by the angular range of the directions of incidence in the convergent beam
- Each direction of incidence produces a point-like diffraction pattern corresponding to the lattice amplitude G with different excitation errors s_z at constant sample thickness

Laboratory for Electron Microscopy

CBED under two-beam conditions: Determination of sample thickness and absorbance length for the excited reflex

Intensity distribution in the diffraction disk given by

$$F^2 \propto G^2 \propto \sin^2 \pi s_{z,eff}\, t$$

$$s_{z,eff} = \sqrt{s_z^2 + \frac{1}{\xi_g^2}}$$

Determination of ξ_g and sample thickness t by analyzing the intensity minima in the Bragg diffraction disk

$$t^2\left(s_k^2 + \frac{1}{\xi_g^2}\right) = n_k^2 \qquad \frac{s_k^2}{n_k^2} = \frac{1}{\xi_g^2 n_k^2} + \frac{1}{t^2}$$

with $$s_k^2 = \frac{\lambda}{d_{hkl}^2} \cdot \frac{\Delta\theta_k}{2\theta_B}$$

s_k : Excitation error at the k-th minimum (k is an integer)
n_k : Counting index for minima

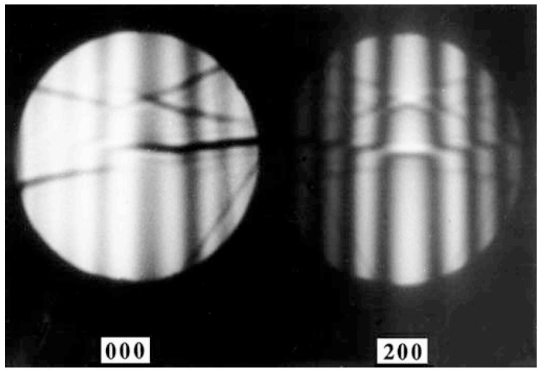

FIGURE 21.6 Parallel Kossel-Möllenstedt fringes in a ZOLZ CBED pattern from pure Al taken under two-beam conditions with (200) strongly excited.

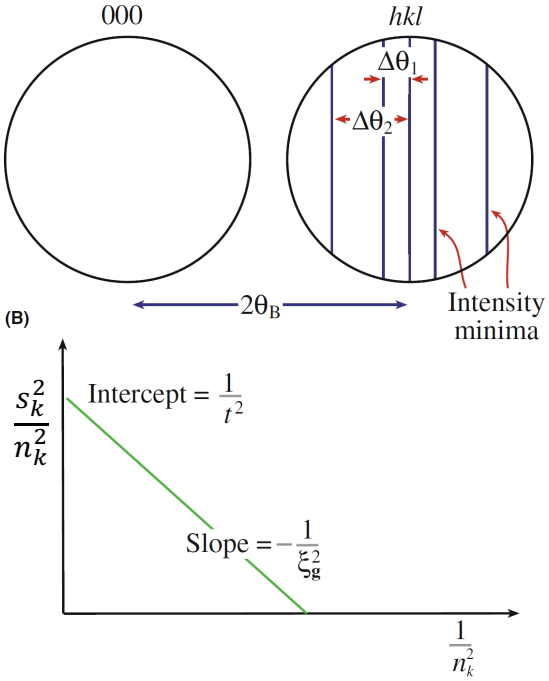

FIGURE 21.8 (A) The measurements necessary to extract thickness (t) from K-M fringes. From n_i measured spacings of $\Delta\theta_i$, determine the deviation parameters s_i, then (B) plot $(s_i/n_k)^2$ against $(1/n_k)^2$. If the plot is a straight line, extrapolate to the ordinate to find t^{-2} and hence t.

Carter&Williams, Figure 21.6, p. 353

Higher Order Laue Zones (HOLZ: Higher Order Laue Zones)

CBED of $MoSe_2$ and MoS_2 in [111] Zone axis with small camera length

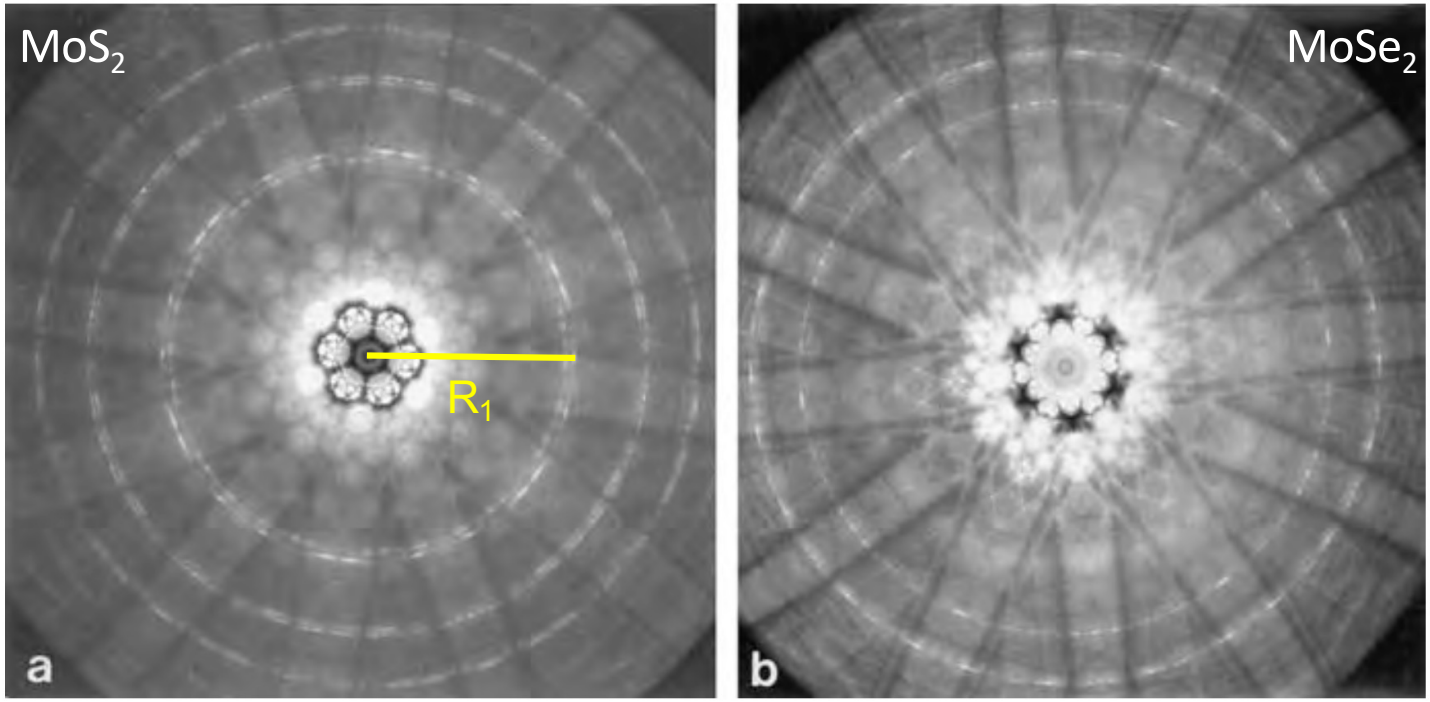

Fig. 8.14. High-order Laue zone (HOLZ) diffraction patterns of 2 H polytypes of (**a**) MoS_2 and (**b**) $MoSe_2$ with structure amplitudes $(f_{Mo} - 1.4f_C)$, f_{Mo}, and $(f_{Mo} + 1.4f_C)$ (C: chalcogen) for the first- to third-order Laue zones, respectively, showing that the first-order Laue zone (FOLZ) of $MoSe_2$ is practically invisible owing to the very small contribution from $(f_{Mo} - 1.4f_{Se})$[8.145].

L. Reimer, Transmission Electron Microscopy, Fig. 9.28

Laboratory for Electron Microscopy

Higher order Laue zones

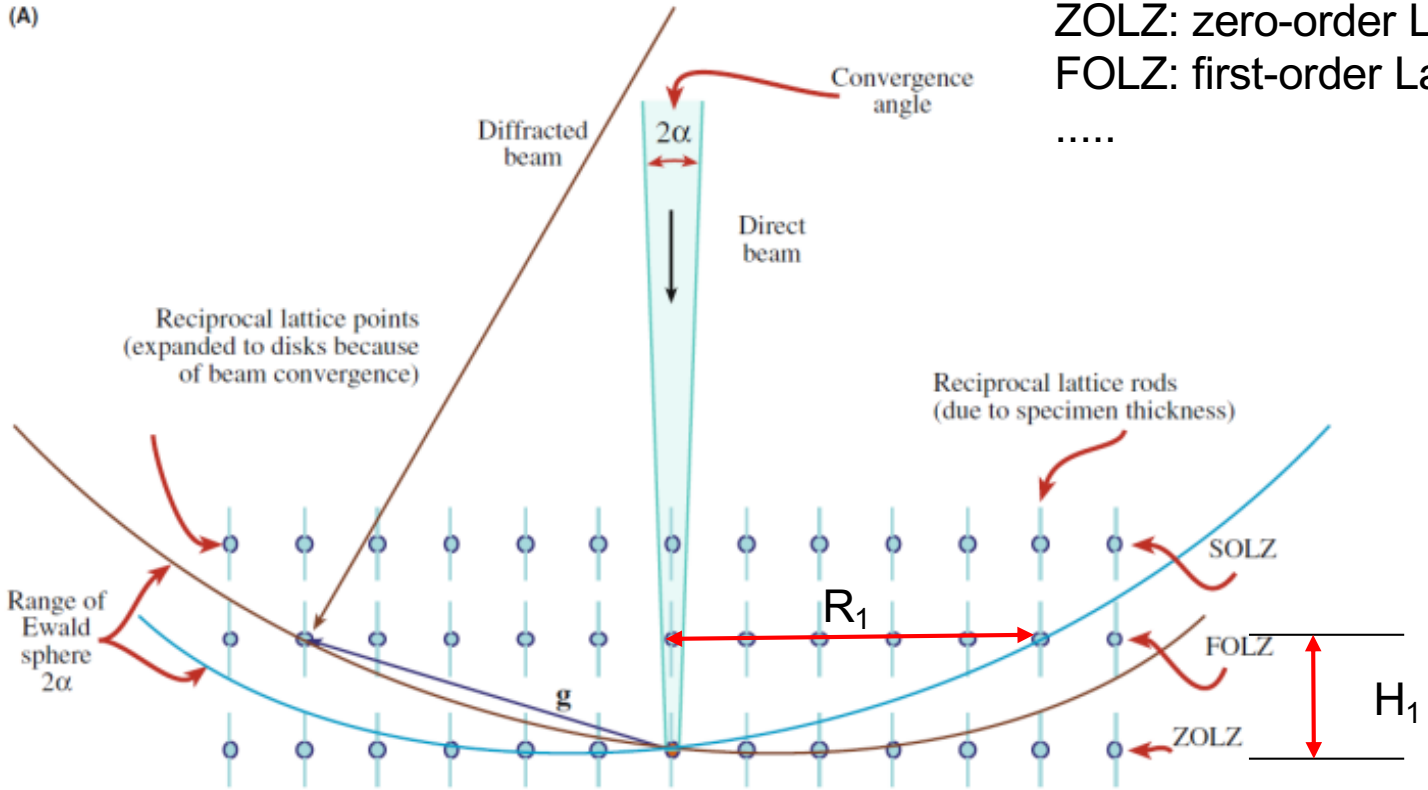

FIGURE 20.11 (A) The Ewald sphere can intercept reciprocal-lattice points from planes not parallel to the electron beam whose **g** vectors are not normal to the beam. The sphere has an effective thickness of 2α because of beam convergence and so intercepts a range of these HOLZ reciprocal-lattice points.

D.B. Williams, C.B. Carter, Transmission Electron Microscopy, Fig. 20.11

ZOLZ: zero-order Laue zone
FOLZ: first-order Laue zone
.....

→ Three-dimensional information about crystal structure
Lattice plane spacing in the direction of transmission

Higher Order Laue Zones (HOLZ)

White's zone law for reflection (hkl) and direction of incidence [UVW] in nth Laue zone

$$hU + kV + lW = n$$

Lattice constant in the direction of incidence from a simple trigonometric view in Ewald Construction:

$$k_0^2 = R_1^2 + (k_0 - H_1)^2 \qquad R_1 = \sqrt{\frac{2H_1}{\lambda}}$$

λ: Wavelength

k_0 : reciprocal wave number

if H_1^2 is negligibly small compared to k_0

$d = 1/H_1$: Lattice plane spacing in the direction of incidence

Laboratory for Electron Microscopy

Kikuchi lines under CBED conditions / HOLZ lines

CBED of silicon in [111] zone axis

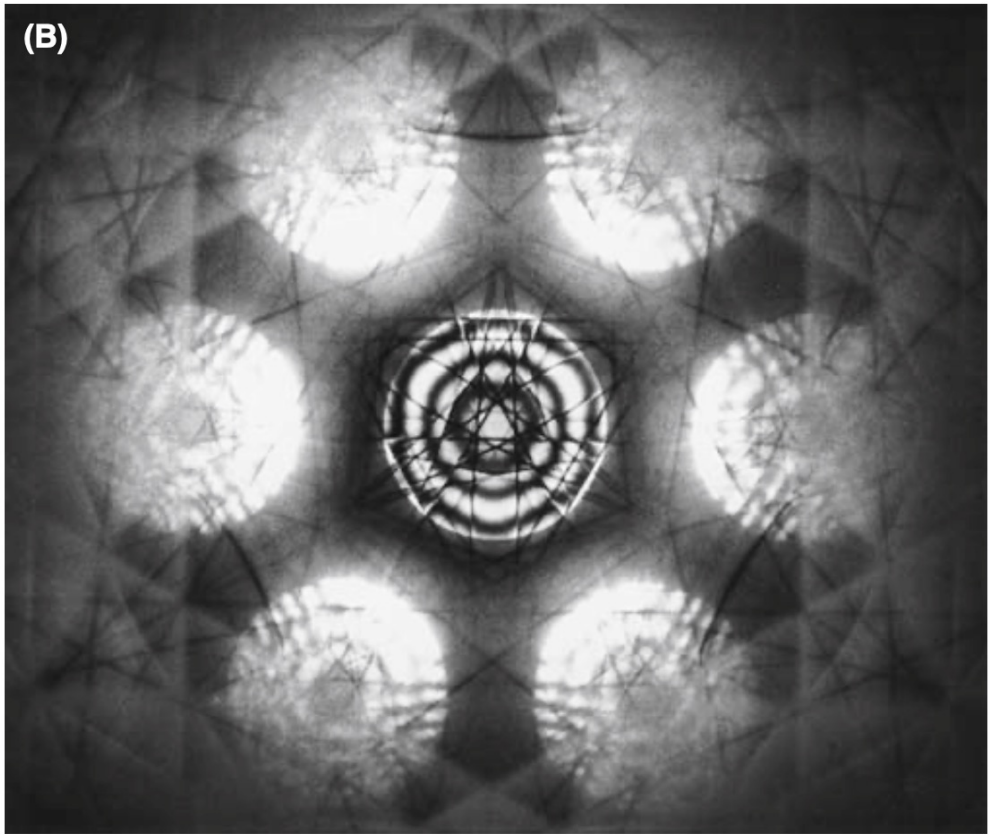

FIGURE 20.2.

(B) CBED pattern from [111] Si showing dynamical contrast within the disks as well as diffuse Kikuchi bands and sharp, deficient HOLZ lines.

D.B. Williams, C.B. Carter, Transmission Electron Microscopy, Fig. 20.2 and Fig. 20.13

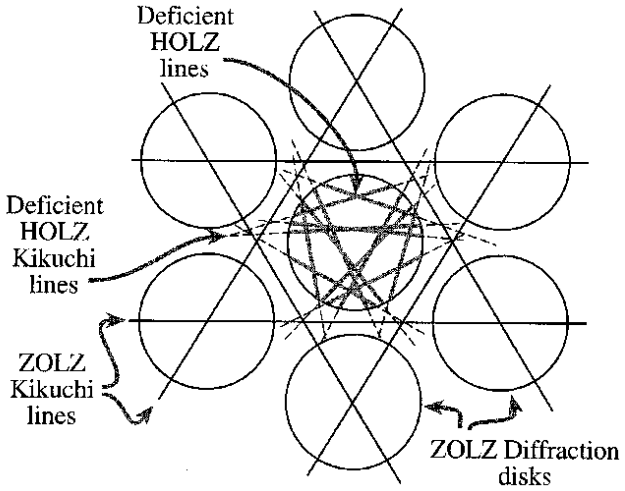

Figure 20.13. The relationship between Kikuchi lines and HOLZ lines is shown in this schematic of a [111] CBED pattern from an fcc crystal. The three principal pairs of $2\bar{2}0$ 110 ZOLZ Kikuchi lines show sixfold symmetry and bisect the g-vectors from 000 to the $2\bar{2}0$ ZOLZ disks. The inelastic HOLZ defect Kikuchi lines are shown in the region between the ZOLZ diffraction disks and the elastic HOLZ defect lines are present within the 000 disk only. Compare this schematic with the experimental pattern back in Figure 20.2B.

Positions of HOLZ Lines (sharp dark lines in the zero beam disk) are very sensitive with regard to:

- Electron energy
- Grid parameters and tensions (local grid parameter changes)

Laboratory for Electron Microscopy

Kikuchi lines under CBED conditions / HOLZ lines

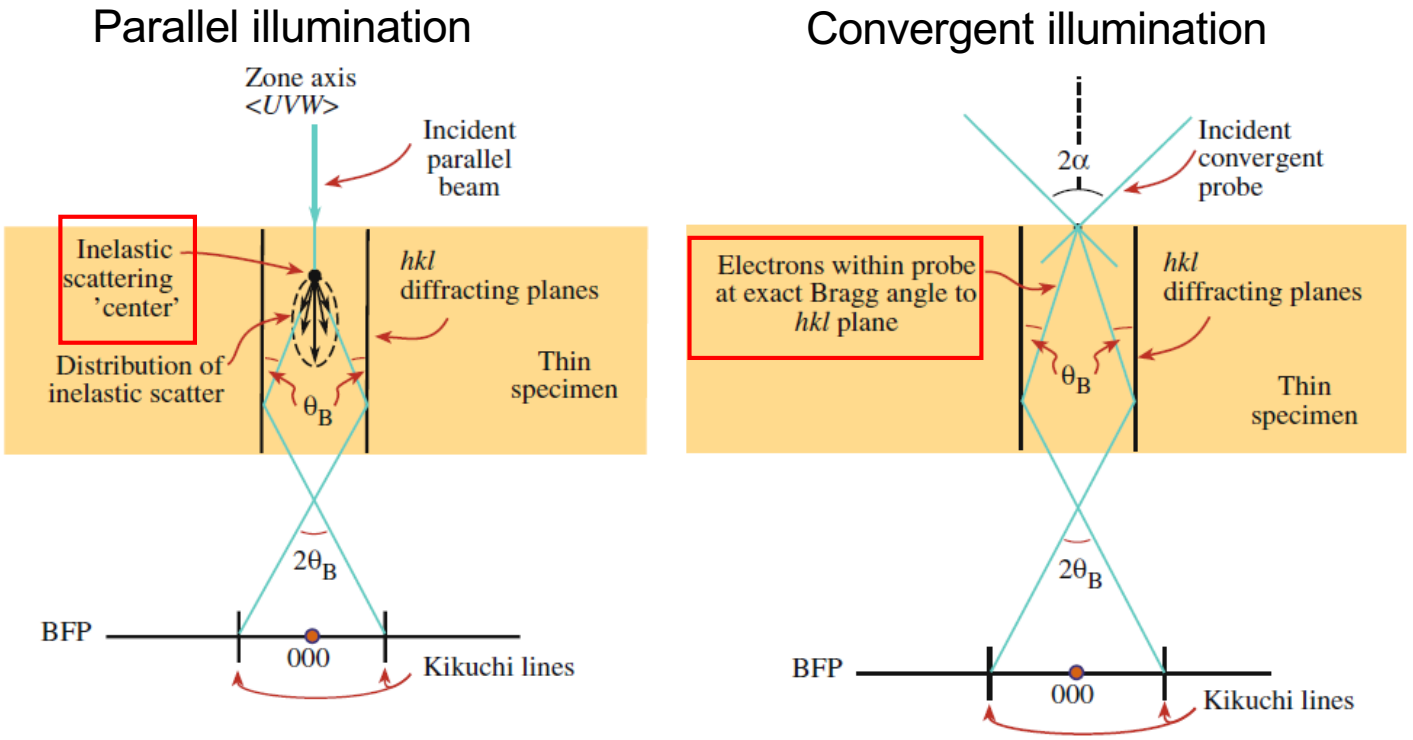

FIGURE 20.14. Comparison of the generation of Kikuchi lines (A) by inelastic scattering of electrons in a parallel beam and (B) by elastic scattering of electrons in a convergent beam when the convergence angle, α is greater than the Bragg angle, θ_B.

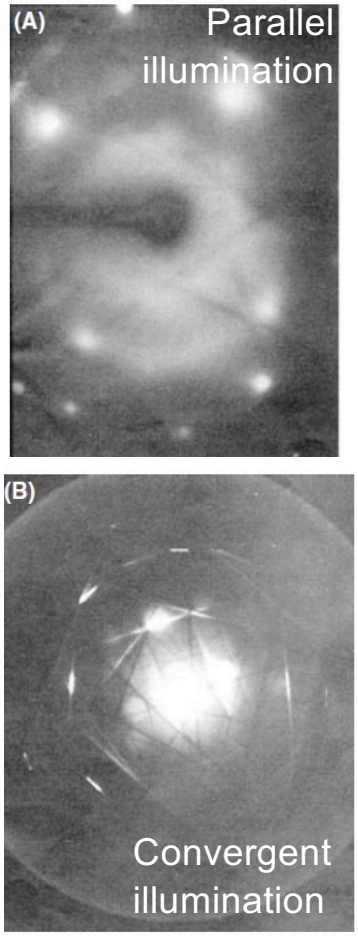

Within diffraction disks: Kikuchi lines <u>without</u> inelastic scattering

⟶ High-contrast and sharp lines even in thin samples

Fulfillment of the Bragg condition for HOLZ reflexes: dark (deficit) lines in the zero beam slice

⟶ Excess lines parallel to this in higher order Laue zones